

(Preprint) AAS 19-806

@ & ' G H 5 H = C B ' ? 5 B 9 D I = J B 9 F ' A G H F 5 H 9 ; < N ' 5 A C 9 F G ' K 9 6 6 ' G D 5 7 9 ' H 9 @ 9 G 7 C D 9

Jeremy Petersen*

The station-keeping plan for the James Webb Space Telescope is zero velocity in the x-component at the fourth successive crossing of the XZ plane of the rotation libration point frame. A differential corrector is employed to determine the necessary delta-v. Maneuvering along the position component of the stable eigenvector of the monodromy matrix produces a minimum delta-v solution. The techniques developed to determine the minimum maneuver direction in a full ephemeris model, along with strategies to cope with the attitude constraints imposed by the sunshield that prevents the ability to maneuver along the stable eigenvector, are examined in this study.

INTRODUCTION

The James Webb Space Telescope (JWST) is a flagship mission scheduled to launch in 2021. It will be the scientific successor to the Hubble Space Telescope and the Spitzer Space Telescope. The project is an international collaboration between the National Aeronautics and Space Administration (NASA), the European Space Agency (ESA), Canadian Space Agency, and NASA Goddard Space Flight Center (GSFC). The JWST mission will focus on the infrared spectrum to detect the redshifted light from very early in the universe, which will fill a gap in the current range of astrophysical observations and allow the exploration of a whole new set of fundamental scientific questions ranging from the formation of the universe to the origin of planetary systems.

Given the sensitivity of the instruments to stray light, the mission will orbit near the Sun-Earth-Moon barycenter (SEMB) L2 libration point, allowing the optical element to remain pointed away from the Sun, the Earth, and the Moon at all times. The near constant geometry of the trajectory relative to the Earth as it orbits about the Sun allows the observatory to map large swaths of the celestial sphere while providing long-duration communication links to the Earth. The orbital dynamics in the L2 region also support the observatory mass-budget constraints with minimal transfer and orbit maintenance costs. Thermal constraints on the instruments impose the need for a 161 square-meter sunshield as show in Figure 1, the presence of which significantly couples the orbital sunshield, thermal requirements also prevent the placement of thrusters on the instrument side of the observatory; consequently, no direct observatory-to-Sun vector maneuver directions are allowed.

* Senior Systems Engineer, Mission Engineering and Technologies Division, a.i. solutions, Inc., 4500 Forbes Blvd. Suite 300, Lanham, MD 20706.

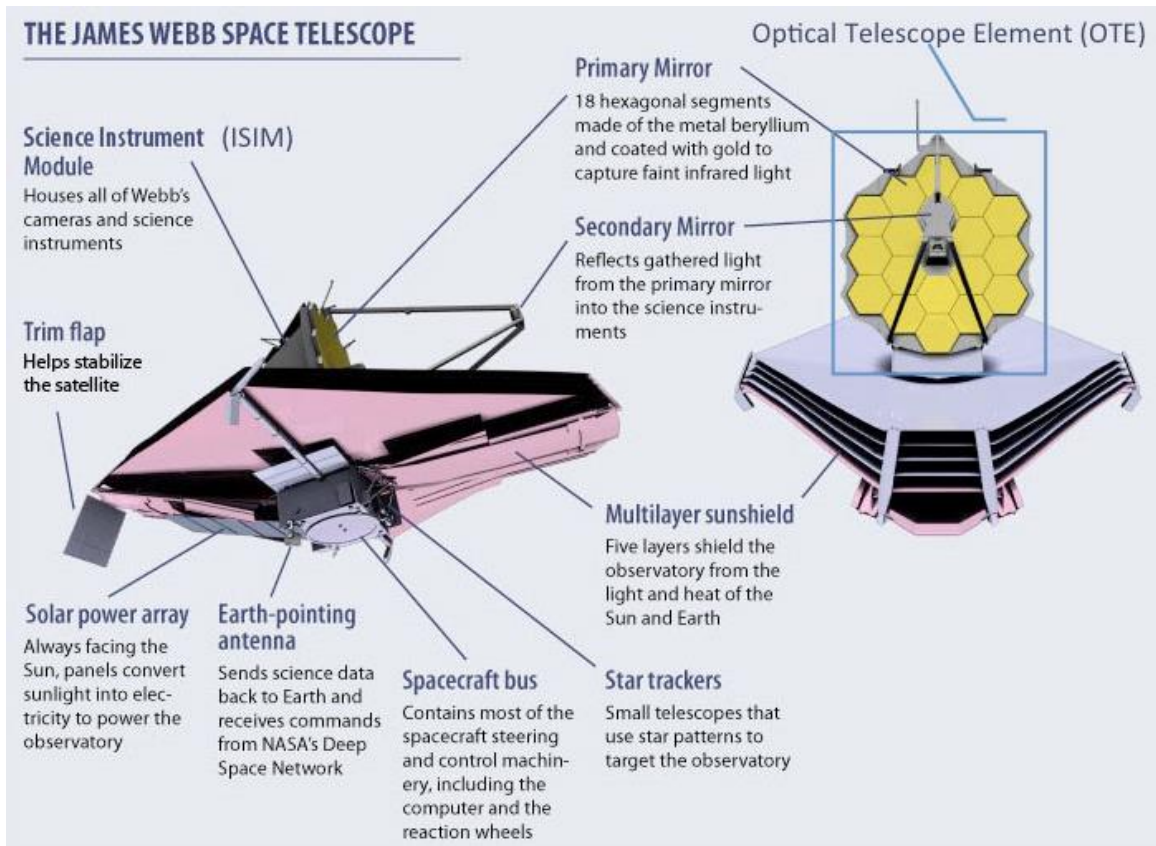


Figure 1. Visual overview of JWST.*

The dynamical region about the SEMB L2 point is inherently unstable. As such, routine station-keeping maneuvers are necessary to keep the observatory in a science orbit for the desired 10.5-year mission lifetime. It is well known that maneuvering along the position components of the stable eigenvector of the monodromy matrix provides the minimum station-keeping delta-v for libration point orbits (LPO).¹⁻³ The present investigation builds on a maneuver strategy implemented for the WIND mission in 2014, which employed maneuvers along the projection of the position components of the stable eigenvector in the ecliptic plane to reduce WIND station-keeping costs between 5 and 25 percent relative to the historical method of maneuvering along the spacecraft-to-Sun line.⁴ The WIND technique will be modified for use by JWST to introduce an out-of-plane component, which will allow for full alignment between the position components of the stable eigenvector and the station-keeping thrust vector. In the event that the attitude restrictions of the observatory prevent alignment between the stable eigenvector and the station-keeping thrust vector, selecting the observatory attitude that places the station-keeping thrust vector as close as possible to the position components of the stable eigenvector will result in the minimum delta-v solution that falls within mission attitude requirements.

STATION-KEEPING DESCRIPTION

There are two types of thrusters on JWST: secondary combustion augments thrusters (SCATs) and monopropellant rocket engine thrusters (MREs). The SCATs are the main thrusters for maneuvering. The SCATs are bi-propellant thrusters and draw from two separate tanks for a hypergolic

* Image credit: <http://jwst.nasa.gov/observatory.html> [accessed 27 June 2019]

reaction. Two pairs of SCATs exist: one for the early orbit mid-course correction maneuvers and one for station-keeping maneuvers. Two pairs are necessary because the center of mass of the observatory changes because of the sunshield deployment between the end of the early orbit mid-course corrections and the beginning of station-keeping maneuvers. Each pair comprises a primary and a redundant thruster. SCAT 1 and 2 are the primary and redundant pair for the early orbit mid-course corrections while SCAT 3 and 4 are the primary and redundant pair for science orbit station-keeping maneuvers. The second set of thrusters is composed of eight dual thruster modules (a.k.a., DTMs), each containing a primary and redundant monopropellant rocket engine (MRE). The MREs provide attitude control during maneuvers and are used for momentum unloading. For a given maneuver, only one SCAT is used throughout the maneuver while the MREs fire intermittently for attitude control.⁵

Station-keeping maneuvers will be performed on a 21-day cadence with the possibility of up to eight momentum unloads throughout each 21-day period. The flight dynamics team is responsible for providing the maneuver plan for station-keeping maneuvers. A maneuver plan consists of a maneuver duration, in seconds, the MJ2000 reference frame orientation of the three observatory body axes at the beginning of the maneuver, and the delta-v vector in MJ2000 reference frame.

The maneuver size and duration are calculated via a differential correction process in the full ephemeris model to determine the maneuver size at a specified direction that achieves zero x-velocity at the fourth crossing of the XZ plane in the rotating libration point (RLP) frame. The x-axis of the RLP frame points from the Sun through the Earth-Moon barycenter, the z-axis points to the north ecliptic pole, and the y-axis completes the right-handed system. The investigation in this paper outlines the method to determine the maneuver direction that minimizes the maneuver size within mission constraints.

LOW-ENERGY MANEUVER SOLUTIONS USING DYNAMICAL SYSTEMS THEORY

Previous studies examined the low-energy based station-keeping solutions for libration point orbits using dynamical systems theory.¹⁻⁴ These studies show that the magnitude of the station-keeping delta-v is minimized by applying the station-keeping delta-v along the position component of the stable eigenvector of the monodromy matrix, as expressed in the RLP frame. The monodromy matrix is generated by propagating state transition matrix for one full revolution around the libration point.

The first step towards the implementation of maneuvering along the stable eigenvector begins with a semi-analytical study employing the well-established circular, restricted, three-body (CR3B) model. The CR3B model, appearing in Figure 2, is a rotating frame composed of three bodies: two primaries, m_1 and m_2 , and an infinitesimally small third body, m_3 . For this application, m_1 is the Sun, m_2 is the Earth-Moon system, and m_3 is JWST. The two primaries orbit about their shared barycenter at a constant angular rate. The x-axis of the frame is defined as the line passing through the two primaries, the z-axis is perpendicular to the plane of rotation, and the y-axis completes the right-handed triad. It is useful to nondimensionalize the equations of motion based on a set of characteristic quantities. The characteristic values for length, mass, and time, are defined as

$$\dots \quad \dots \quad \frac{\mu}{m_1 + m_2} \quad (1)$$

where D_1 and D_2 are the distances between the primaries and their barycenter, m_1 and m_2 are the masses of the primaries, and G is the dimensional gravitation constant.

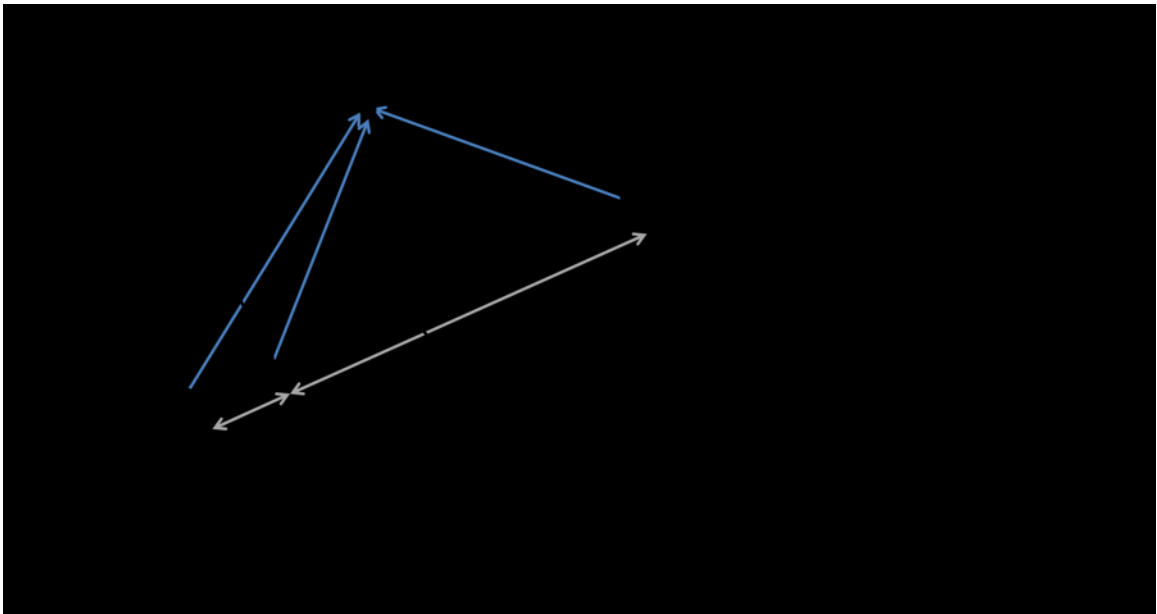


Figure 2. Circular, restricted, three-body model definition.

Using the characteristic quantities defined above, the nondimensional time parameter, t , and mass parameter, μ , are defined as

$$\dots \dots \dots \quad (2)$$

and the nondimensional vectors describing the position of the spacecraft relative to the two primaries, \mathbf{r}_1 and \mathbf{r}_2 , and relative to the barycenter of the system, \mathbf{r} , are defined as

$$\dots \dots \dots \quad (3)$$

The unit vectors \mathbf{e}_1 , \mathbf{e}_2 , and \mathbf{e}_3 are the axes of the rotating frame.

With the nondimensional quantities established, the equations of motion for the third body in the system is

$$\dots \dots \dots \quad (4)$$

where the dots represent differential with respect to nondimensional time. U^* is the pseudo-potential function,

$$\dots \dots \dots \quad (5)$$

where d and r are scalar distances,

$$\dots \dots \dots \quad (6)$$

The low-energy maneuver direction is along the position components of the stable eigenvector of the monodromy matrix. To calculate this matrix, the state transition matrix, Φ , associated with the CR3B equations of motions must be numerically integrated for one period about the libration point. The first order differential equation governing the state transition matrix is

(7)

where $A(t)$ is the Jacobian matrix that is composed of the partial derivatives of the equations of motion, $\dot{\mathbf{x}}$, with respect to each of the six states, \mathbf{x} ,

(8)

For the case study presented in this investigation, a launch epoch of January 14, 2021, at 12:10 UTC is selected. The resulting orbit for this launch epoch is a tight quasi-halo with a maximum RLP-Y and RLP-Z amplitude of approximately 771,000 km and 418,000 km, respectively. The distance between the Sun and the Earth-Moon barycenter in the CR3B model was set to a mean distance of 149.5e6 km. Figure 3 provides a comparison between the representative CR3B halo orbit and the full ephemeris quasi-halo orbit at the instance of the selected launch epoch. The green orbit represents the CR3B halo orbit while the black orbit represents the full ephemeris model quasi-halo orbit propagated for 10.5 years past launch.

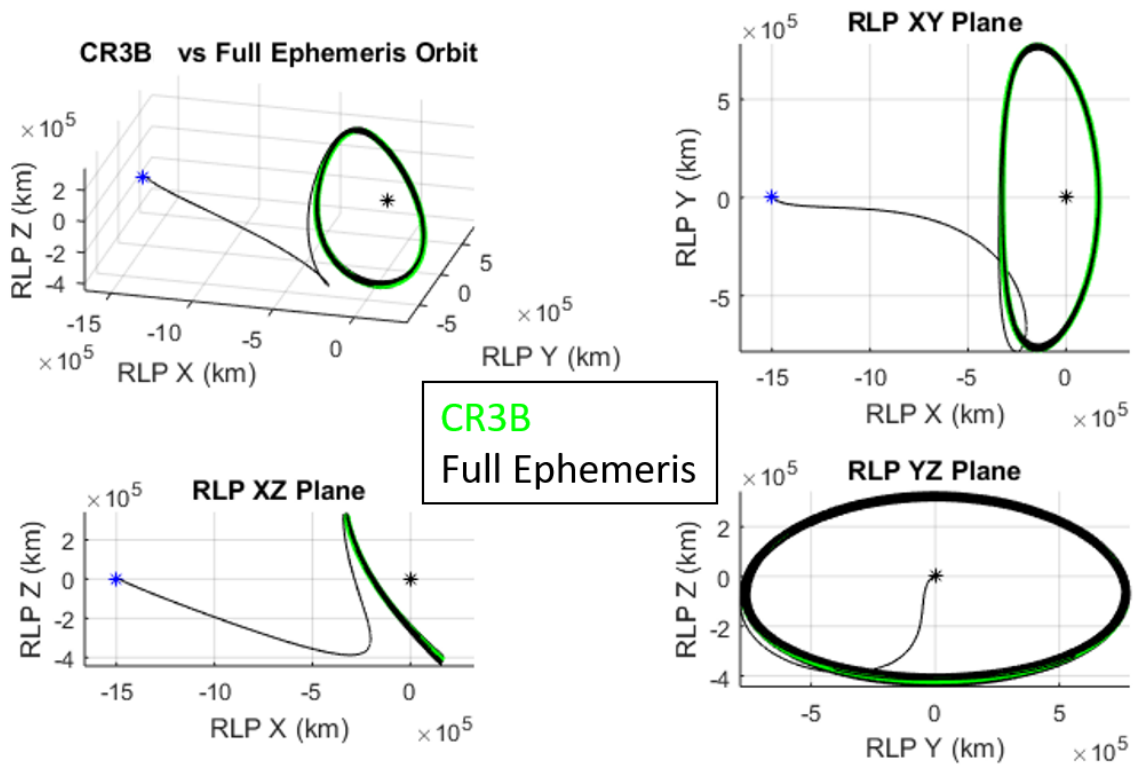


Figure 3. Visualization of the reference halo orbit used for this investigation. The maximum RLP-Y and RLP-Z amplitude is approximately 771,000 km and 418,000 km, respectively.

With a representative orbit selected in the CR3B model, the monodromy matrix can be constructed at various locations throughout the representative orbit and the direction of the stable eigenvector can be calculated through an eigenvalue decomposition of each monodromy matrix. For this representative halo orbit, only two of the six eigenvalues contain only a real component; one eigenvalue corresponds to a stable mode and the other to the unstable mode. As such, the eigenvector associated with the singular stable eigenvalue is the eigenvector that determines the direction of the low-energy delta-v solution. Figures 4 and 5 show two representations of the position components of stable eigenvector calculated in the CR3B regime. Figure 4 shows the position components of the stable eigenvector at various locations throughout the representative orbit. Figure 5 constructs the stable eigenvector direction into a series of two angles as a function of the orbit angle in the RLP-XY plane: the angle of the stable eigenvector in the RLP-XY plane and the angle of the stable eigenvector out of the RLP-XY plane.

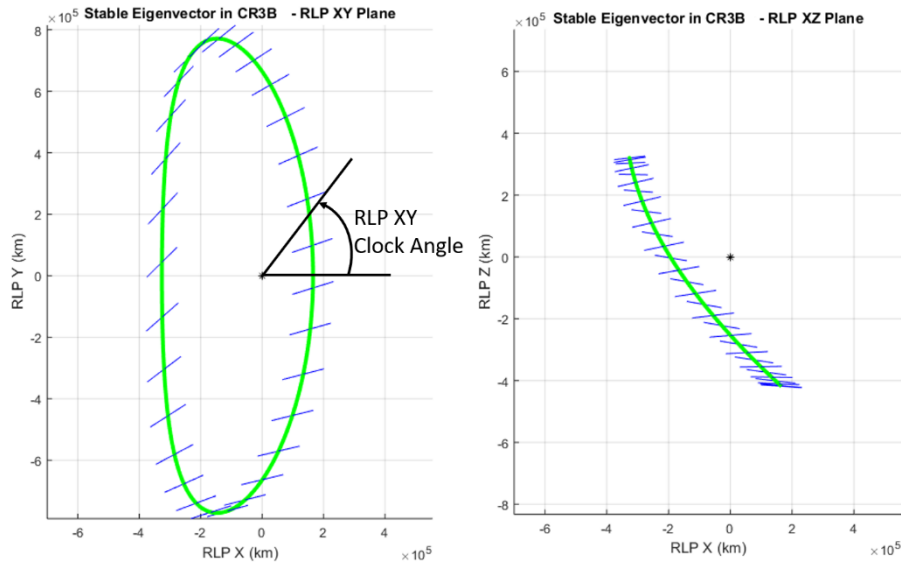


Figure 4. The direction of the stable eigenvector, in blue, in the RLP frame throughout various orbit locations in the reference halo orbit in the CR3B problem. The Sun is located along the \hat{E}_x axis.

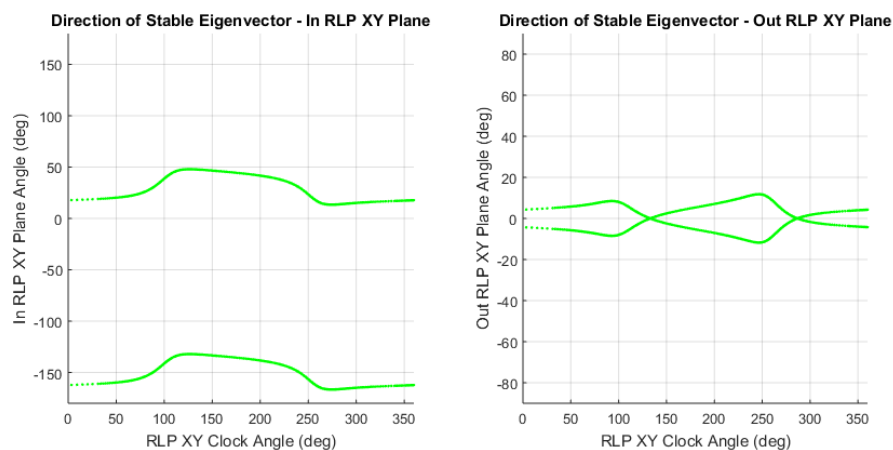


Figure 5. Representation of the stable eigenvector in terms of an RLP-XY in-plane angle and RLP-XY out-of-plane angle. Both angles are a function of location in the RLP-XY plane.

As seen in the left plot in Figure 5, the direction of the position components of the stable eigenvector in the CR3B model is either in the first quadrant (0 to 90 degrees) or third quadrant (̄180 to ̄90 degrees) in the RLP-XY planar projection. The out-of-plane component of the stable eigenvector is within ± 10 degrees of the ecliptic plane. Maneuvering along or near the stable eigenvector in the first quadrant of the RLP-XY plane is denoted as an anti-sunward maneuver while maneuvering along or near the stable eigenvector in the third quadrant is donated as a sunward maneuver (although the observatory cannot maneuver directly toward the Sun).

TECHNIQUE TO FIND THE STABLE EIGENVECTOR IN THE FULL EPHEMREIS MODEL

During the investigation into the minimization of WIND maneuver sizes, it was noted that the station-keeping delta-v size as a function of the angle of the direction of the maneuver in the RLP-XY plane creates a straight line when plotted in a polar representation.⁴ An example of this behavior from the WIND study appears in Figure 6. The angle in the polar plot in Figure 6 represents the direction of the delta-v applied in the RLP-XY plane relative to the RLP +x-axis. The delta-v magnitude is measured radially and is in units of m/s. The blue line was constructed by calculating the maneuver size that converges on a perpendicular fourth crossing of the RLP-XZ plane for a range of maneuver directions between 0 and 90 degrees off the RLP +x-axis in 10-degree increments. The region between 0 and 90 degrees corresponds to the quadrant that contains the position components of the stable eigenvector. For a given planar scan, either in the RLP-XY plane or out of the RLP-XY plane, the low-energy delta-v solution for that plane is calculated by finding the line starting at the origin that is perpendicular to the line representing the delta-v size as a function of maneuver direction angle. For this WIND example, maneuvering in the direction of the low-energy delta-v solution saved approximately 9 cm/s of delta-v, which is a 20% improvement relative to the legacy strategy of directing the delta-v along the spacecraft-to-Sun vector in the RLP-XY plane.

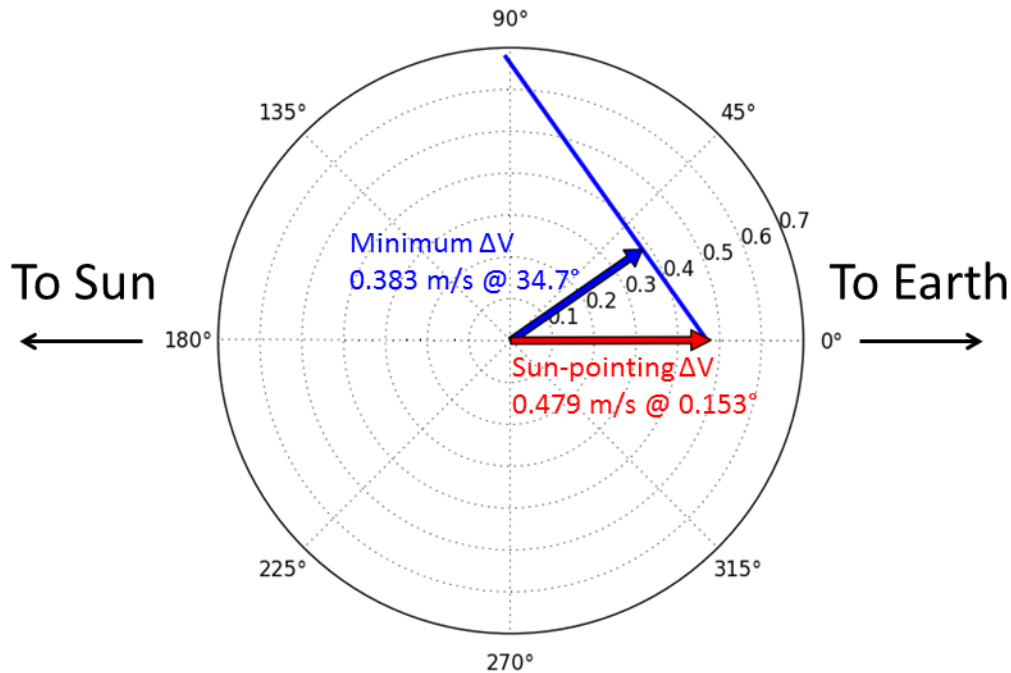


Figure 6. Example of the minimization technique that was developed for WIND.⁴ Maneuver magnitude is measured radially in units of m/s while the maneuver direction in the RLP-XY plane is the angle in the polar plot and is in units of degrees.

Because the definition of a line only requires two points, a shortcut can be employed to calculate the line representing the delta-v sizes as a function of maneuver direction by calculating two data points comprised of both maneuver magnitude and angle. Two maneuver directions are selected with the only requirement that both directions must point in the same quadrant of the RLP plane to ensure the maneuver sign is the same for both data points. For a scan in the RLP-XY plane, directions in either quadrant 1 for anti-sunward maneuver or quadrant 3 for sunward maneuvers are acceptable. For the scan out of the RLP-XY plane, quadrant 1 is acceptable for both sunward and anti-sunward maneuvers. With the directions selected, a differential correction process is applied to calculate the maneuver size necessary to achieve a perpendicular crossing with zero x-velocity at the fourth crossing of the RLP-XZ axis in the full ephemeris model.

The two data points necessary to construct the line of delta-v costs, represented by the red and green dots in Figure 7, are first represented in polar space as a function of maneuver direction angle, θ_i , and maneuver magnitude, r_i . The polar coordinates can be transformed into cartesian space through a simple transformation.

$$x_i = r_i \cos \theta_i \quad y_i = r_i \sin \theta_i \quad (9)$$

With the two data points defined in Cartesian space, the slope, m_{DV} , and y-intercept, b_{DV} , of the line created by the two points, represented by the blue line in Figure 7, can be calculated.

$$m_{DV} = \frac{y_2 - y_1}{x_2 - x_1} \quad b_{DV} = \frac{y_1 - m_{DV} x_1}{1} \quad (10)$$

With the slope, m_{DV} , and intercept, b_{DV} , of the line known, the slope of the line starting at the origin and perpendicular to the delta-v cost line represented in Figure 7 by the orange line, m_T , is the inverse reciprocal of m_{DV} . The y-intercept of the perpendicular line, b_T , will be zero as the orange line is required to pass through the origin. The minimum delta-v solution will be the intersection of the two lines.

$$x_{min} = \frac{-b_{DV}}{m_{DV} - m_T} \quad y_{min} = m_T x_{min} \quad (11)$$

The Cartesian solution, x_{min} and y_{min} , can be converted back into a polar coordinates, which provides the minimum maneuver magnitude, r_{min} , and associated maneuver direction, θ_{min} .

$$r_{min} = \sqrt{x_{min}^2 + y_{min}^2} \quad \theta_{min} = \arctan\left(\frac{y_{min}}{x_{min}}\right) \quad (12)$$

WIND is only able to adjust the maneuver direction in the RLP-XY plane as its spin axis is oriented along the south ecliptic pole.⁴ JWST, on the other hand, can adjust the delta-v vector both within and out of the RLP-XY plane. As part of this investigation, it was observed that the linear relationship between maneuver angle and maneuver magnitude in the RLP-XY plane also exists when adjusting the maneuver direction out of the RLP-XY plane, as long as the angle in the RLP-XY plane remains constant. The plot on the left in Figure 7 illustrates an example of the station-keeping maneuver magnitudes for a given angle from the x-axis in the RLP-XY plane. The plot on the right in Figure 7 shows an example of extending the scanning direction out of the RLP-XY plane while keeping the RLP-XY in-plane angle constant at the angle of the minimum solution found in the RLP-XY in-plane scan. The black star in the right plot on Figure 7 represents the minimum delta-v solution.

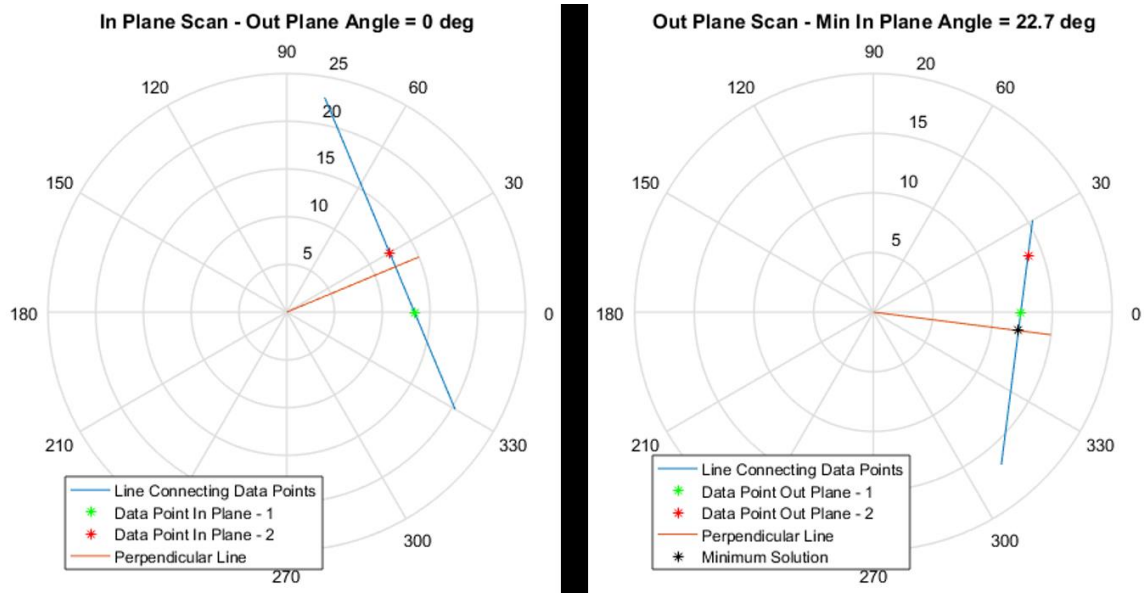


Figure 7. Linear solving technique for JWST. The left polar plot shows results in the RLP-XY plane while the right polar plot shows the results out of the RLP-XY plane. The maneuver direction in the given plane, in degrees, is measured by the angle in the polar plot. Delta-v magnitude, measured radially, is in units of cm/s.

The linear relationship leads to a simple algorithm to quickly determine the lowest delta-v solution at any point in a libration point orbit using only four differential correction processes, two in-plane and two out-of-plane. The process works in either a CR3B regime or one based on planetary ephemerides. The results of a brute-force scan across a range of in-plane and out-of-plane angles appear in Figure 8. Overlaid in Figure 8 is the result from the simple algorithm, confirming that it results in the lowest delta-v.

The station-keeping algorithm was tested numerically at multiple orbit locations to ensure robustness. Figure 9 replicates the direction of the position components of the stable eigenvector in the CR3B regime (from Figure 5) in green, with the addition of the black stars that represent the low delta-v solution direction calculated using the algorithm at a variety of orbit locations in the full ephemeris model. As expected, there is excellent agreement between the location of the position components of the stable eigenvector in the CR3B model and the direction of the low delta-v solution calculated in the full ephemeris model. Because they are essentially coincident, going forward, the [lowest delta-v solution] and the [stable eigenvector X] f Y Wh] c b [k] V Y i g Y X ably.

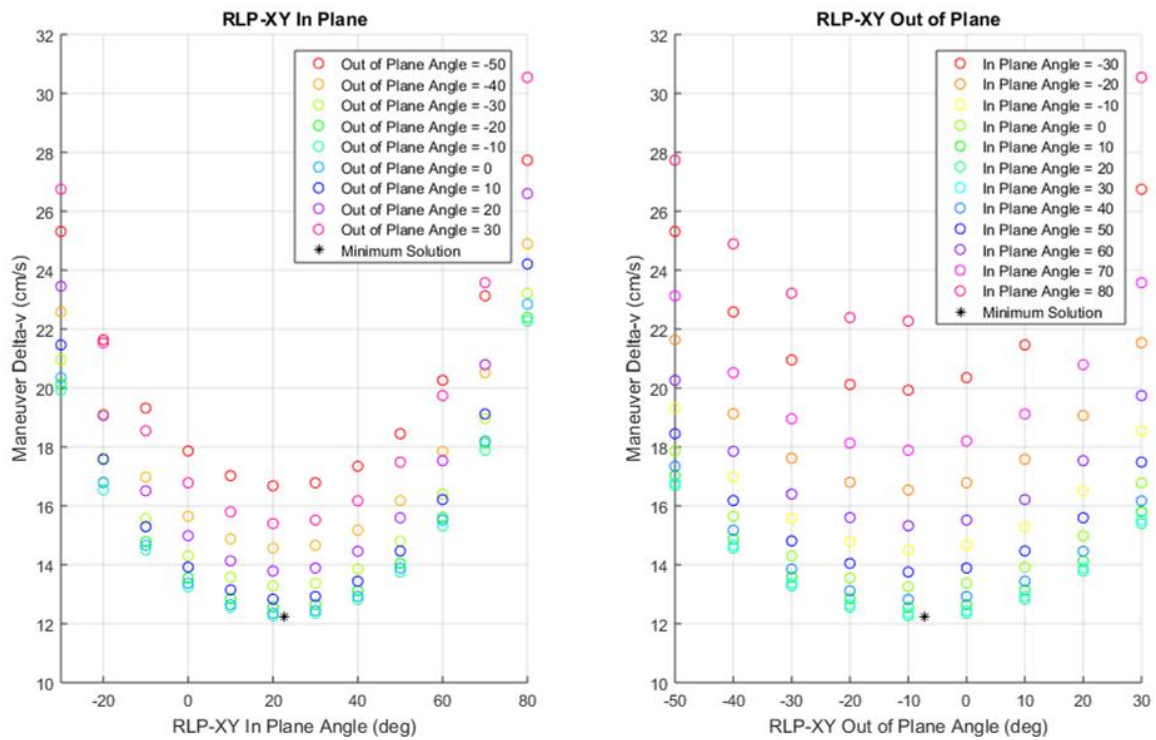


Figure 8. Brute force scan to demonstrate success finding the minimum delta-v solution, as noted by the black star, using only four differential correction process.

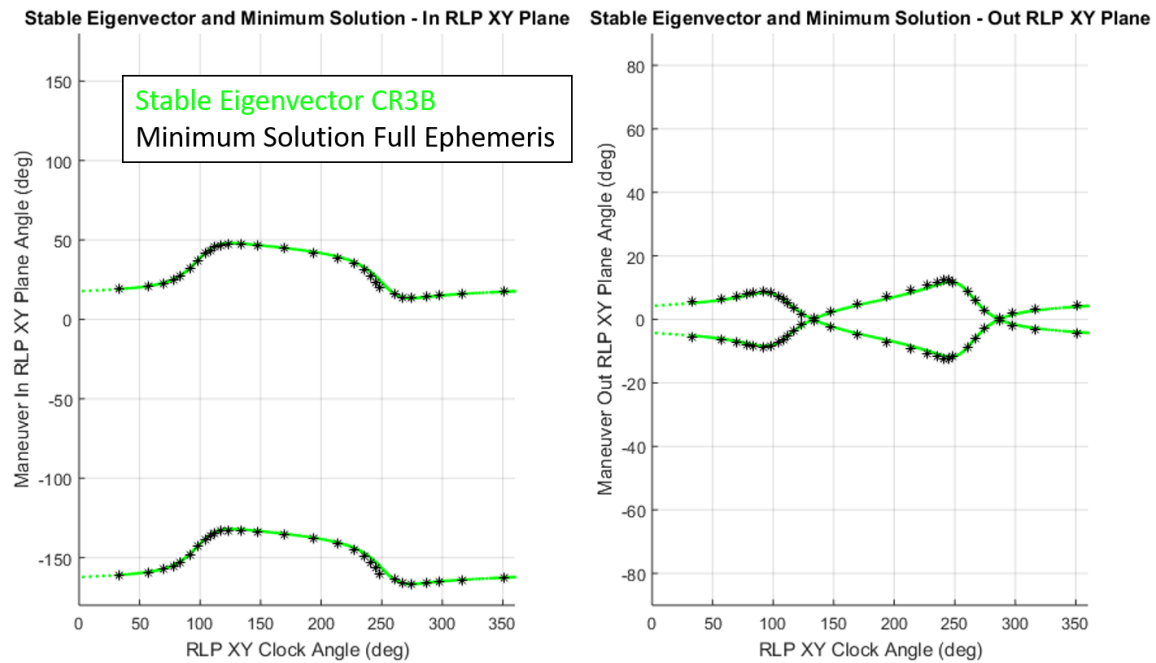


Figure 9. Confirmation that the minimum delta-v solution aligns with the stable eigenvector. The green lines are the stable eigenvectors calculated in the CR3B model while the black stars are minimum delta-v solutions found at various orbit locations.

Figure 13. Alternative definition describing the orientation of the primary station-keeping thrust vector in terms of RLP-XY in-plane angle and RLP-XY out-of-plane angle.

The limitations imposed by the allowable range of Sun angles necessitates an additional step in the maneuver planning process to generate a suitable maneuver plan. After the direction of the position components of the stable eigenvector has been determined, the Sun angles necessary to align the station-keeping thrust vector with the stable eigenvector direction are calculated. If the calculated Sun angles satisfy requirements, then the low-energy delta-v solution along the position components of stable eigenvector will be used to construct the maneuver plan. If the calculated Sun angles do not fall within requirements, which will be the majority of station-keeping maneuvers, an additional step is necessary to determine the allowable Sun pitch and Sun yaw combination that minimizes the maneuver delta-v: the station-keeping thrust vector is oriented as close as possible to the stable eigenvector.

For anti-sunward maneuvers and when the station-keeping thrust vector cannot be aligned with the stable eigenvector, the Sun pitch that orients the thrust vector as close as possible to the stable eigenvector will always be 0 degrees. For a sunward maneuver, because it is impossible to align the station-keeping thrust vector and stable eigenvector, the Sun pitch will always be ± 53 degrees. This simplifies the search process as Sun yaw becomes the only free variable. The Sun yaw, at a fixed Sun pitch of 0 degrees for an anti-sunward maneuver or ± 53 degrees for a "sunward" maneuver, that minimizes the vertex angle between the stable eigenvector and the resulting station-keeping thrust vector orientation will result in the minimum delta-v size that falls within mission requirements.

The Sun yaw that produces the minimum vertex angle between the stable eigenvector and station-keeping thrust vector appears in Figure 14; this yaw results in the minimum delta-v solution within attitude constraints and will be a unique value for various locations throughout the orbit. The top half of Figure 14 illustrates an example of a result from a specific location along the trajectory for an anti-sunward maneuver while the bottom half provides an example for a sunward maneuver.

For the anti-sunward half of Figure 14 (top row of plots), the results are straightforward. A sinusoidal relationship is apparent between the vertex angle and Sun yaw. This relationship produces a minimum delta-v cost around a Sun yaw of 70 degrees for this specific orbit location, which corresponds to the minimum vertex angle as well.

The results for the sunward half (bottom row of plots) of Figure 14 are more complicated. Because of the large range of potential in-plane and out-of-plane orientations for the station-keeping thrust vector, as seen in Figures 11 and 12, the sinusoidal relationship crosses the boundary set by the unstable eigenvector, resulting in both positive and negative delta-v values for the range of Sun yaws studied. A negative delta-v value corresponds to an observatory attitude that places the station-keeping thrust vector in the anti-sunward direction, at which point a negative impulsive delta-v is necessary to achieve the desired sunward maneuver (and violating the attitude constraints). The values of Sun yaw that produce a negative impulsive delta-v are not a valid attitude for the station-keeping maneuver. For the Sun yaw values that do produce a positive delta-v, the same relationship regarding the Sun yaw, vertex angle, and minimum delta-v solutions exists. For this specific location along the trajectory, the Sun yaw that produces the minimum delta-v is ± 10 degrees.

Figure 14. Demonstration that when the station-keeping thrust vector cannot align with the stable eigenvector, the Sun yaw value (at a fixed Sun pitch value of 0 degrees for anti-sunward maneuver and ± 53 degrees for sunward maneuver) that minimizes the angle between the station-keeping thrust

vector and stable eigenvector will result in the lowest delta-v solution within allowable attitude constraints.

To further illustrate the importance of selecting the correct Sun yaw to help minimize the delta-v costs for JWST, Figure 15 illustrates the percent increase in the maneuver size relative to the low-energy delta-v solution along the position components of the stable eigenvector as a function of Sun yaw. For this anti-sunward maneuver example, the percent increase for the minimum solution within attitude constraints relative to the minimum solution along the stable eigenvector is only a few percent, if the right Sun yaw angle is selected; however, selecting the wrong Sun yaw value results in a maneuver plan up to double the size of the best-case yaw value and needlessly wastes fuel. The potential for wasting fuel is even more apparent in the sunward example. Because sunward maneuvers are limited to the RLP-YZ plane, the angle between the stable eigenvector and the thrust vector orientation is quite large no matter the value of Sun yaw. The vertex angle range for anti-sunward maneuvers, apparent in Figure 14, is between 15 and 60 degrees. The range in vertex angle for sunward maneuvers is much larger, between 65 and 115 degrees. The minimum vertex angle in the sunward case is 65 degrees, which results in significant efficiency loss when maneuvering in the sunward direction. The efficiency loss is illustrated numerically in Figure 15 as the best Sun yaw solution within attitude constraints still results in a 200% increase in maneuver size relative to maneuvering along the position components of the stable eigenvector in the sunward direction. Because of the attitude constraints for JWST, this efficiency loss is unavoidable for a sunward maneuver; however, the efficiency loss can be mitigated as best as possible through selection of the correct Sun yaw value during the maneuver planning process.

Figure 15. Maneuver size relative to the minimum solution along the stable eigenvector as a function of maneuver Sun yaw. The Sun pitch is fixed at 0 degrees for anti-sunward maneuvers or -53 degrees for sunward maneuver.

CONCLUSION

The delta-v minimization technique first implemented by WIND to find the direction of the stable eigenvector in the RLP-XY plane is extended to include a component out of the RLP-XY plane to find the direction of the stable eigenvector in all three RLP dimensions. To find the direction of the stable eigenvector for an arbitrary location in a libration point orbit, four differential correction processes, two in-plane and two out-of-plane, are necessary. With the direction of the stable eigenvector known, the Sun angles necessary to align the station-keeping thrust vector and

the stable eigenvector are calculated. If the resulting Sun angles fall within requirements, the maneuver direction will be along the stable eigenvector and result in a low delta-v solution maneuver plan. In the event that the resulting Sun angles do not fall within requirements, a Sun yaw value is calculated that minimizes the distance between the stable eigenvector and resulting station-keeping thrust vector orientation with the Sun pitch fixed at 0 for anti-sunward maneuvers and 53 degrees for sunward maneuvers. Selection of a proper Sun yaw for a maneuver plan is critical to ensure that the station-keeping maneuvers remain as efficient as possible when oriented away from the position components of the stable eigenvector.

ACKNOWLEDGMENTS

U"] " ' g c ` i h] c b g Ð ' Wc b h f] V i h] c b ' h c ' NNG14VC09C.c f _ ' k U g ' 0

REFERENCES

¹Folta, D. C., Pavlak, T. A., Howell, K. C., Woodard, M. A., and Woodfork, D. M., "Stationkeeping of Lissajous Trajectories in the Earth-Moon System with Applications to ARTEMIS," 20th AAS/AIAA Space Flight Mechanics Meeting, San Diego, CA, February, 2010.

²Pavlak, T. A., and Howell, K. C., "Strategy for Long-Term Libration Point Stationkeeping in the Earth-Moon System," AAS/AIAA Astrodynamics Specialist Conference, Girdwood, AK, August, 2011.

³Folta, D., Woodard, M., Pavlak, T., Haapala, A., and Howell, K., "Earth-Moon Libration Stationkeeping: Theory, Modeling, and Operations," *Acta Astronautica* Vol. 94, No. 1, January-February 2014, Pages 421-433, ISSN 0094-5765.

4. 6 f c k b ž ' > " ' A " ž ' D Y h Y f g Y b ž ' > " ' ? " ž ' [5 d d ` m] b [' 8 m b U a] W U ` ' G m g h Y a g A U b Y i j Y f g ' Z c f ' K = B 8 ž Ā ' 5 = 5 5 # 5 5 G ' 5 g h f c X m b U a] W g ' G d Y W] U `] g h ' 7 c b

5. Peterseb ž ' > " ž ' H] W \ m ž ' > " ž ' K U k f n m b] U _ ž ' ; ž ' U b X ' - C o r r e c t i o n ? " ž ' [> U a Y g A c b h Y ' 7 U f ` c ' = a d ` Y a Y b h U, 24th International Symposium on Space Flight Dynamics, Laurel, Maryland, May 2014.

